Yearly variation in characteristics and health risk of polycyclic aromatic hydrocarbons and nitro-PAHs in urban shanghai from 2010–2018

Lu Yang[1], Xuan Zhang[1], Wanli Xing[1], Quanyu Zhou[1], Lulu Zhang[1], Qing Wu[2], Zhijun Zhou[2], Renjie Chen[2], Akira Toriba[3], Kazuichi Hayakawa[4], Ning Tang[3,4,*]

[1] Graduate School of Medical Sciences, Kanazawa University, Kakuma-machi, Kanazawa, 920-1192, Japan

[2] School of Public Health, Fudan University, Shanghai 200032, China

[3] Institute of Medical, Pharmaceutical and Health Sciences, Kanazawa University, Kakuma-machi, Kanazawa, 920-1192, Japan

[4] Institute of Nature and Environmental Technology, Kanazawa University, Kakuma-machi, 920-1192, Kanazawa, Japan

ABSTRACT

This study encompassed the regular observation of nine polycyclic aromatic hydrocarbons (PAHs) and three nitro-PAHs (NPAHs) in particulate matter (PM) in Shanghai in summer and winter from 2010 to 2018. The results showed that the mean concentrations of ΣPAHs in summer decreased by 24.7% in 2013 and 18.1% in 2017 but increased by 10.2% in 2015 compared to the data in 2010. However, the mean concentrations of ΣPAHs in winter decreased by 39.7% from 2010 (12.8 ± 4.55 ng/m^3) to 2018 (7.72 ± 3.33 ng/m^3), and the mean concentrations of 1-nitropyrene in winter decreased by 79.0% from 2010 (42.3 ± 16.1 pg/m^3) to 2018 (8.90 ± 2.09 pg/m^3). Correlation analysis with meteorological conditions revealed that the PAH and NPAH concentrations were both influenced by ambient temperature. The diagnostic ratios of PAHs and factor analysis showed that they were mainly affected by traffic emissions with some coal and/or biomass combustion. The ratio of 2-nitrofluoranthene to 2-nitropyrene was near 10, which indicated that the OH radical-initiated reaction was the main pathway leading to their secondary formation. Moreover, backward trajectories revealed different air mass routes in each sampling period, indicating a high possibility of source effects from the northern area in winter in addition to local and surrounding influences. Meanwhile, the mean total benzo[a]pyrene-equivalent concentrations in Shanghai in winter decreased by 50.8% from 2010 (1860 ± 645 pg/m^3) to 2018 (916 ± 363 pg/m^3). These results indicated the positive effects of the various policies and regulations issued by Chinese authorities.

© 2020 The Research Center for Eco-Environmental Sciences, Chinese Academy of Sciences. Published by Elsevier B.V.

Introduction

Atmospheric particulate matter (PM) plays a major role in air pollution. PM can not only change the climate at the global and re-

gional scales (Byambaa et al., 2019; Zhang et al., 2020a) but can also exert harmful effects on human health (Feng et al., 2019; Polachova et al., 2020) related to a variety of toxic compounds (Wang et al., 2017). Polycyclic aromatic hydrocarbons (PAHs, consisting of two and/or more fused benzene rings) are a class of ubiquitous toxic organic species (Baek et al., 1991) that are well known for their carcinogenicity and/or mutagenicity (Nisbet and Lagoy, 1992). As nitro derivatives of PAHs, nitro-PAHs (NPAHs) have become a concern because they exhibit a more profound direct-acting mutagenicity than PAHs (Taga et al., 2005). Most NPAHs originate directly from incomplete burning, similar to PAHs (Harrison et al., 1996), while several kinds of NPAHs, such as 2-nitropyrene (2-NP) and 2-nitrofluoranthene (2-NFR), are generated in the atmosphere via secondary formation between their parent PAHs and NO_2 (Arey et al., 1986; Zielinska et al., 1989).

Due to the rapid development of urbanization and industrialization, China has experienced serious atmospheric pollution (Jiang et al., 2018; Tang et al., 2017; Zhang et al., 2019a, Zhang et al., 2020a). Shanghai is one of the largest economic centres in China, located in the Yangtze Delta Region in eastern China, with a total area of 6340 km^2 and a population of over 24 million. The health risks to humans caused by PM inhalation exposure are particularly important due to the high population density of Shanghai (Liu et al., 2017; Wang et al., 2019). To our knowledge, much reporting on environmental pollution in Shanghai has focused on PAHs and NPAHs. However, such reports have focused only on certain events, such as the World Expo (Wang et al., 2014), and on certain periods, such as wet deposition periods (Yan et al., 2012), or on seasonal variations within one year (Liu et al., 2018; Wang et al., 2016a; Zhang et al., 2019b). Although mid-to-long-term observation is important and necessary because it is beneficial to clarify the variations in pollutants in nature (concentration, composition, etc.) and emission sources in the regional atmosphere, such mid-to-long-term research on PAHs in PM in China is still very limited (Kong et al., 2018; Wang et al., 2015; Yang et al., 2019). Moreover, only our previous study reported the characteristics of mid-to-long-term changes in NPAHs in Beijing from 2004 to 2010 (Tang et al., 2017). To our knowledge, the characteristics of mid-to-long-term changes in PM-bound PAHs and NPAHs in Shanghai have not yet been reported. Therefore, after the observation of PAHs and NPAHs in 2010 (Tang et al., 2013), we regularly collected PM samples at the same site in Shanghai in summer and winter from 2013 to 2018.

We determined the concentrations of 9 PM-bound PAHs and 3 PM-bound NPAHs. The data were also compared to our past results from samples collected at the same site in 2010 (Tang et al., 2013). The main objectives were (1) to clarify the variations in the concentrations, compositions, and health risks of PM-bound PAHs and NPAHs; (2) to clarify the correlation between PAHs and NPAHs and meteorological conditions; and (3) to determine the emission sources based on the diagnostic ratios, factor analysis, and backward trajectory analysis.

1. Materials and methods

1.1. PM sampling

As shown in Fig. 1, PM sampling was performed in the School of Public Health, Fudan University (31.2°N, 121.4°E), located in Xuhui District, which is the central area in Shanghai, China. The sampling site was approximately 500 m away from the main road. The PM sampler was set up on the rooftop of a five-floor building.

The PM samples with aerodynamic diameters > 2.1 μm ($PM_{>2.1}$) and ≤ 2.1 μm ($PM_{\leq 2.1}$) were separately collected by a low-volume air sampler (AN-200, Sibata Scientific Technology Ltd., Japan) loaded onto quartz fibre filters (2500QAT-UP, Pall Co., USA). The flow rate was 28.3 L/min. PM samples were collected in summer (Aug. 8 to 20, 2013 ($n = 5$), Jun. 1 to 18, 2015 ($n = 6$) and Jul. 8 to 22, 2017 ($n = 7$)) and winter (Dec. 13 to 27, 2013 ($n = 6$), Dec.

Table 1 – Information on each individual PAH and NPAH.

Species	Abbreviation	Ring number	MW[a]	TEF$_i$ [b]
Fluoranthene	FR	4	202.3	0.001
Pyrene	Pyr	4	202.3	0.001
Benz[a]anthracene	BaA	4	228.3	0.1
Chrysene	Chr	4	228.3	0.01
Benzo[b]fluoranthene	BbF	5	252.3	0.1
Benzo[k]fluoranthene	BkF	5	252.3	0.1
Benzo[a]pyrene	BaP	5	252.3	1
Benzo[ghi]perylene	BgPe	6	276.3	0.01
Indeno[1,2,3-cd]pyrene	IDP	6	276.3	0.1
1-Nitropyrene	1-NP	4	247.3	0.1
2-Nitropyrene	2-NP	4	247.3	-[c]
2-Nitrofluoranthene	2-NFR	4	247.3	0.05

[a] MW means molecular weight (g/mol).
[b] TEF$_i$ means toxic equivalent factor. The values of nine PAHs are from Nisbet and Lagoy, 1992; 1-NP from OEHHA, 2005; 2-NFR from Durant et al., 1996.
[c] No TEF value.

25, 2015 to Jan. 8, 2016 ($n = 6$) and Jan. 5 to 19, 2018 ($n = 7$)). After sampling, each filter was packaged in aluminium foil and kept in sealed plastic bags for storage at -25°C until analysis.

1.2. Experimental analysis of the PAHs and NPAHs

The pretreatment of filters is similar to that in a previous study (Xing et al., 2020). Briefly, the PM filters ($PM_{>2.1}$ and $PM_{\leq 2.1}$) were cut into several pieces. Pyrene-d_{10} (Pyr-d_{10}, 98%, Wako Pure Chemicals, Osaka, Japan) and benzo[a]pyrene-d_{12} (BaP-d_{12}, 98%, Wako Pure Chemicals, Osaka, Japan) were added to the samples as internal standards before extraction. After ultrasonic extraction, the solutions were filtered, and the extracts were successively washed with a dilute NaOH (97%, Wako Pure Chemicals, Osaka, Japan) solution (5%, W/V), H_2SO_4 (98%, Wako Pure Chemicals, Osaka, Japan) solution (20%, v/v), and distilled water. Then, the solutions were concentrated and filtered into vials. After pretreatment, nine PAHs and three NPAHs (Table 1) in each PM sample were detected by a high-performance liquid chromatography (HPLC, LC-20AD, Shimadzu Inc., Kyoto, Japan) system. The detailed detection method is shown in the Supplementary Material (**Appendix A Text S1**) (Tang et al., 2011).

In this study, the US EPA 610 PAH mix standard (99%) was procured from Supelco Park (Bellefonte, PA, USA), 1-NP (98%) and 2-NP (98%) were purchased from Aldrich Chemical Company (Osaka, Japan), and 2-NFR (99%) was acquired from Chiron AS (Trondheim, Norway). All other reagents (analytical reagent grade) used in HPLC analysis were purchased from Wako Pure Chemicals (Osaka, Japan).

1.3. Quality control and quality assurance

To measure the background contamination during transportation, blank filters were also analysed. No target chemicals were determined, indicating that no contamination occurred during transport. The calibration curves of nine PAHs and three NPAHs all showed good linearity ($r > 0.998$), and the relative standard deviations ($n = 3$) of nine PAHs and three NPAHs were within 5%. Internal standards were used to quantify the PAHs and NPAHs. The recoveries of internal standards in all samples ranged from 80% to 103% in this study. The limit of determination and the range of calibration curves of each PAH and NPAH are shown in **Appendix A Table S1**.
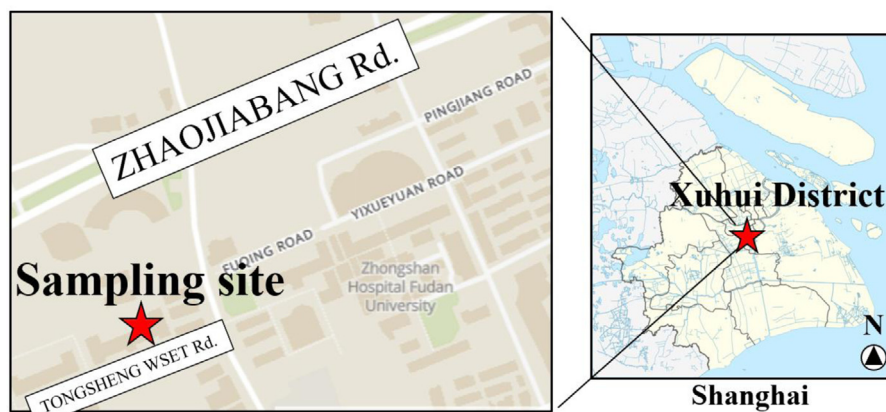
Fig. 1 – Location of the sampling site in Shanghai, China.

1.4. Data analysis

1.4.1. Meteorological conditions

Meteorological conditions including average ambient temperature, relative humidity, precipitation, and average wind speed during the sampling periods were obtained from the NNDC Climate Data Online (https://www7.ncdc.noaa.gov/CDO/cdo). **Appendix A Table S3** summarizes the mean value and standard deviation of meteorological conditions.

1.4.2. Backward trajectory analysis

The air masses during the sampling period were analysed based on the backward trajectory method with the U.S. National Oceanic and Atmospheric Association's HYSPLIT4 model (WINDOWS-based). In this study, backward trajectories were calculated every hour, and the duration time was 24 hr (marked every 6 hr) at a sampling point height of 500 m above ground level; this height has been found to have the largest influence on the PM in Shanghai (Liu et al., 2018; Zhang et al., 2019b). All backward trajectories were classified into 3 or 4 clusters according to their characteristics of the spatial trajectory distribution during each sampling period.

1.4.3. Health risk assessment

The potential health risk of PAHs is often expressed by the BaP-equivalent concentration (BaP_{eq}) (Eq. (1)) and the inhalation lifetime cancer risk (ILCR) (Eq. (2)):

$$BaP_{eq} = \sum (C_i \times TEF_i) \tag{1}$$

$$ILCR = UR_{BaP} \times BaP_{eq} \tag{2}$$

where, C_i (pg/m³) is each individual PAH and NPAH concentration, and TEF_i is the toxic equivalent factor of each individual PAH, 1-NP, and 2-NFR (Table 1) relative to BaP (Durant et al., 1996; Nisbet and Lagoy, 1992; OEHHA, 2005). UR_{BaP} is the unit cancer risk from BaP; as the value of 8.7×10^{-5} per ng/m³ used in this study was determined by the WHO in an epidemiological study of coke-oven workers (WHO World Health Organization, 2000).

1.4.4. Statistical analysis

IMB SPSS version 25.0 was used for statistical analysis of the data. In this study, the K-S (Kolmogorov-Smirnov) test showed that the concentrations of ΣPAHs and ΣNPAHs in summer and winter from 2013 to 2018 were normally distributed. The correlations of PAHs, NPAHs and meteorological conditions were determined by Pearson correlation analysis. A p value less than 0.05 indicated that the results were significant. Principal component analysis (PCA) can reveal high loadings of certain variables on a given factor, thereby simply and clearly identifying the various emission sources of PAHs (Ravindra et al., 2008).

2. Results and discussion

2.1. Concentrations and compositions of the PM-bound PAHs and NPAHs

The mean PAH and NPAH concentrations in $PM_{\leq 2.1}$ from 2010 to 2018 are listed in Table 2. The ΣPAHs and ΣNPAHs concentrations in $PM_{\leq 2.1}$ accounted for 71% to 87% of the total concentrations ($PM_{\leq 2.1} + PM_{>2.1}$, **Appendix A Table S2**), indicating higher levels of PM-bound PAHs and NPAHs in fine particles. Because fine particles more easily penetrate the respiratory system, causing various diseases in humans (Dunea et al., 2016), this paper mainly focused on the analysis of PAHs and NPAHs in $PM_{\leq 2.1}$.

Table 2 indicates that the mean concentrations of ΣPAHs in $PM_{\leq 2.1}$ in summer did not change substantially and were relatively high in 2015 (1.83 ± 1.11 ng/m³) and low in 2013 (1.25 ± 0.51 ng/m³). In winter, compared to the data obtained in 2010 (12.8 ± 4.55 ng/m³) (Tang et al., 2013), the mean concentrations of ΣPAHs slightly increased in 2013 (14.2 ± 8.44 ng/m³) and then decreased in 2015 (9.51 ± 4.18 ng/m³) and 2018 (7.72 ± 3.33 ng/m³) (Table 2). The nine ΣPAHs concentration levels in summer and winter were both matched with the results reported by Liu et al. (2017) in Shanghai in 2014 (2.46 ng/m³ in summer and 11.6 ng/m³ in winter). These concentrations were comparable to those in Nanjing in 2013/2014 (2.99 ng/m³ in summer and 13.2 ng/m³ in winter) (Kong et al., 2018) but much lower than those in other central and northern cities, such as Wuhan in 2014 (10.34 ng/m³ in summer and 40.6 ng/m³ in winter) (Zhang et al., 2019c), Jinan in 2016 (7.55 ng/m³ in summer and 56.2 ng/m³ in winter) (Zhang et al., 2019d), Beijing in 2015 (7.81 ng/m³ in summer and 214 ng/m³ in winter) (Zhang et al., 2020b), and Shenyang from 2012 to 2014 (19.7 ng/m³ in summer and 153 ng/m³ in winter) (Yang et al., 2019). Based on the data contained in Table 2, the proportions of 4-, 5- and 6-ring PAHs (Table 1) in summer in each year each accounted for approximately one-third of ΣPAHs, while in winter, the order changed slightly to 4-ring > 5-ring > 6-ring PAHs. The dominant PAHs in $PM_{\leq 2.1}$ were mostly BbF, BgPe, and IDP in summer and mostly FR, BbF, and BgPe in winter (Table 2). These results suggest that the differences in ΣPAHs concentrations may be related to meteorological conditions and emission sources, which will be discussed in detail in Sections 2.2 and 2.3.

Regarding the NPAHs, in summer, Table 2 reveals that compared with 2010 (Tang et al., 2013), the mean concentrations of

Table 2 – Mean PAH (ng/m³) and NPAH (pg/m³) concentrations in PM$_{\leq 2.1}$ from 2010 to 2018*.

	2010[a]		2013		2015		2017/2018	
	Summer	Winter	Summer	Winter	Summer	Winter	Summer	Winter
FR	0.11 ± 0.05	1.17 ± 0.65	0.14 ± 0.05	2.06 ± 1.29	0.22 ± 0.11	1.57 ± 0.53	0.15 ± 0.04	1.39 ± 0.92
Pyr	0.12 ± 0.05	0.96 ± 0.46	0.13 ± 0.04	1.86 ± 1.06	0.22 ± 0.09	1.09 ± 0.32	0.11 ± 0.01	0.85 ± 0.58
BaA	0.05 ± 0.02	0.99 ± 0.44	0.06 ± 0.03	0.68 ± 0.46	0.07 ± 0.04	0.56 ± 0.26	0.06 ± 0.01	0.51 ± 0.29
Chr	0.11 ± 0.04	1.74 ± 0.76	0.12 ± 0.04	1.64 ± 1.02	0.11 ± 0.07	0.93 ± 0.44	0.09 ± 0.02	0.83 ± 0.40
BbF	0.29 ± 0.08	2.14 ± 0.84	0.21 ± 0.10	2.10 ± 1.23	0.34 ± 0.22	1.62 ± 0.80	0.27 ± 0.04	1.32 ± 0.43
BkF	0.11 ± 0.02	0.89 ± 0.30	0.07 ± 0.03	0.81 ± 0.47	0.11 ± 0.07	0.65 ± 0.32	0.07 ± 0.02	0.47 ± 0.16
BaP	0.15 ± 0.03	1.27 ± 0.45	0.10 ± 0.05	1.14 ± 0.73	0.12 ± 0.08	0.66 ± 0.36	0.11 ± 0.01	0.58 ± 0.25
BgPe	0.43 ± 0.13	2.19 ± 0.89	0.30 ± 0.14	2.53 ± 1.49	0.35 ± 0.25	1.39 ± 0.78	0.27 ± 0.05	0.98 ± 0.27
IDP	0.28 ± 0.09	1.45 ± 0.57	0.13 ± 0.06	1.36 ± 0.79	0.28 ± 0.19	1.05 ± 0.55	0.22 ± 0.05	0.80 ± 0.22
ΣPAHs	1.66 ± 0.50	12.8 ± 4.55	1.25 ± 0.51	14.2 ± 8.44	1.83 ± 1.11	9.51 ± 4.18	1.36 ± 0.20	7.72 ± 3.33
2-NFR	-[b]	-[b]	-[b]	-[b]	93.0 ± 68.4	316 ± 211	174 ± 86.6	169 ± 70.3
2-NP	-[b]	-[b]	-[b]	-[b]	7.76 ± 5.88	35.9 ± 28.2	9.45 ± 4.73	24.7 ± 17.3
1-NP	6.28 ± 2.81	42.3 ± 16.1	3.49 ± 1.09	30.8 ± 15.4	1.91 ± 0.77	11.7 ± 6.42	4.29 ± 1.24	8.90 ± 2.09
ΣNPAHs	-[c]	-[c]	-[c]	-[c]	103 ± 74.9	363 ± 244	187 ± 91.3	202 ± 73.3

* Concentration = mean ± standard deviation.
[a] Data from Tang et al., 2013.
[b] Not analysed.
[c] Only 1-NP concentration.

1-NP in 2013 (3.49 ± 1.09 pg/m³) and 2015 (1.91 ± 0.77 pg/m³) decreased slightly but increased in 2017 (4.29 ± 1.24 pg/m³), while in winter, the mean concentrations of 1-NP gradually decreased 79.0% from 2010 (42.3 ± 16.1 pg/m³) to 2018 (8.90 ± 2.09 pg/m³). Table 2 also indicates that the 2-NP concentration variation was similar to that in 1-NP. However, the concentration of 2-NFR in PM$_{\leq 2.1}$ in summer was higher than that in winter in 2017/2018, which differed from 1-NP (Table 2). Previous studies also showed a similar result: the 2-NFR and/or 2-NP concentrations in cold seasons were lower than those in warm seasons in some Asian cities (Kameda et al., 2004). This occurs because the atmospheric 2-NFR and/or 2-NP depend not only on their parent PAH concentrations but also on meteorological conditions (temperature, solar radiation, etc.) and other air pollutants (NO$_x$, O$_3$, etc.) (Albinet et al., 2008).

2.2. Correlations between PAHs, NPAHs, and meteorological conditions

It has been previously reported that in addition to emission sources from human activities (local and/or external), the generation, accumulation, diffusion, removal, and phase partitioning of air pollutants are influenced by meteorological conditions (Amarillo and Carreras, 2016; Wang et al., 2016b). Table 3 summarizes the correlations between the meteorological conditions and the individual PAHs and NPAHs in PM$_{\leq 2.1}$ in the sampling periods.

Table 3 lists the significant negative correlations between the temperature and each individual PAH, 1-NP, and 2-NP ($p <$ 0.05 and/or $p <$ 0.01), indicating that the concentration was relatively high when the temperature was low. **Appendix A Table S3** reveals that the mean temperature in winter was approximately 16 to 27°C lower than that in summer. It has been reported that PAHs with more than 4-rings can be transferred from the gaseous phase to the particle phase at relatively low ambient temperatures due to the low vapour pressure (Yamasaki et al., 1982). This was one of the reasons for the higher proportion of 4-ring PAHs in winter than in summer described in Section 2.1. On the other hand, the height of the mixed layer in Shanghai is relatively low and stable in winter, hindering the dispersion of air pollutants originating from human activities and thus resulting in high PAH concentrations (Gu et al., 2010).

Table 3 – Correlations between meteorological conditions and the individual PAHs and NPAHs in PM$_{\leq 2.1}$ during the sampling periods.

	Temperature	Precipitation	Relative humidity	Wind speed
P	0.06	1.00	0.37*	−0.18
RH	−0.20	0.37*	1.00	−0.27
WS	0.16	−0.18	−0.27	1.00
FR	−0.78**	−0.18	−0.11	0.01
Pyr	−0.74**	−0.14	−0.09	−0.02
BaA	−0.78**	−0.19	−0.14	0.00
Chr	−0.74**	−0.16	−0.10	−0.04
BbF	−0.76**	−0.20	−0.04	−0.10
BkF	−0.76**	−0.19	−0.02	−0.14
BaP	−0.70**	−0.17	−0.11	−0.06
BgPe	−0.65**	−0.17	−0.03	−0.13
IDP	−0.73**	−0.20	−0.01	−0.14
2-NFR	−0.26	−0.32	−0.20	−0.36
2-NP	−0.44*	−0.25	0.10	−0.35
1-NP	−0.59**	−0.15	−0.08	−0.12

* means correlation is significant at $p < 0.05$;
** means correlation is significant at $p < 0.01$.

Although previous studies reported that precipitation, relative humidity, and wind speed had negative correlations with air pollutants (Jiang et al., 2018; Kakimoto et al., 2000; Wang et al., 2016b), the data in Table 3 did not indicate any significant negative correlations with each individual PAH and NPAH in this study. This may have occurred because there was nearly no precipitation during the sampling periods in addition to summer in 2015 (Appendix A Table S3). Meanwhile, the variation in wind speed was not large in each sampling period in this study (Appendix A Table S3).

2.3. Emission sources of PAHs and NPAHs

The PAH diagnostic ratios are commonly used for the identification of potential emission sources, and several diagnostic ra-

Table 4 – Diagnostic ratios of PAHs and NPAHs in PM$_{\leq 2.1}$ from 2010 to 2018.

	Coal and/or biomass burning	Traffic emission	2010[e]		2013		2015		2017/2018	
			Summer	Winter	Summer	Winter	Summer	Winter	Summer	Winter
[FR]/([FR] + [Pyr])	> 0.5[a]	0.4 - 0.5[a]	0.48	0.55	0.52	0.53	0.49	0.59	0.56	0.62
[BaA]/([BaA] + [Chr])	> 0.35[b]	0.22 - 0.55[b]	0.34	0.36	0.33	0.29	0.40	0.37	0.43	0.38
[BaP]/[BgPe]	> 0.5[c]	0.2 - 0.5[c]	0.36	0.58	0.35	0.45	0.35	0.47	0.42	0.59
[IDP]/([IDP] + [BgPe])	> 0.6[d]	< 0.6[d]	0.40	0.40	0.31	0.35	0.44	0.43	0.44	0.45
[2-NFR]/[1-NP]			-[f]	-[f]	-[f]	-[f]	48.7	27.1	40.5	19.0
[2-NFR]/[2-NP]			-[f]	-[f]	-[f]	-[f]	12.0	8.79	18.4	6.82

[a] Rogge et al., 1993
[b] Simcik et al., 1999
[c] Yang et al., 2019
[d] Yunker et al., 2002.
[e] Data from Tang et al., 2013.
[f] No data.

tios in PM$_{\leq 2.1}$ from 2010 to 2018 and referenced data on emission sources are summarized in Table 4. Compared to the referenced data (Rogge et al., 1993; Simcik et al., 1999; Yang et al., 2019; Yunker et al., 2002), the [BaP]/[BgPe] and [IDP]/([IDP] + [BgPe]) ratios indicated traffic emissions, while the [FR]/([FR] + [Pyr]) and [BaA]/([BaA] + [Chr]) ratios indicated mixed traffic emissions and coal and/or biomass combustion, although there were only slight differences between periods.

The diagnostic ratio of [2-NFR]/[1-NP] can not only estimate the relative importance of the secondary formation and primary emission of NPAHs into the atmosphere but can also estimate the exposure time of atmospheric NPAHs (Bamford and Baker, 2003). As revealed in Table 4, all ratios higher than 5 indicated the relative importance of the secondary formation of 2-NFR. However, a lower ratio was observed in winter than in summer, suggesting that the effect of primary emissions was larger in winter. Moreover, the low ambient temperature and weak solar radiation in winter hinder the photochemical degradation of 1-NP, resulting in relatively low [2-NFR]/[1-NP] ratios (Tang et al., 2014). The diagnostic ratio of [2-NFR]/[2-NP] was applied to determine whether the main formation pathway of the NPAHs was the OH radical-initiated reaction (value close to 10) or the NO$_3$ radical-initiated reaction (value close to 100) (Bamford and Baker, 2003). Table 4 shows that all ratios of [2-NFR]/[2-NP] were close to 10, suggesting that the main secondary formation pathway of 2-NFR and 2-NP in Shanghai was the OH radical-initiated reaction.

PCA was also conducted to identify the emission sources in summer and winter, and the loadings of each individual PAH in PM$_{\leq 2.1}$ are listed in Table 5. In this study, only 2 factors (PC1 and PC2) were examined because they explained 92.1% and 93.1% of the total variance in summer and winter, respectively. PC1 had high loadings for 5- and 6-ring PAHs, and PC2 had high loadings for FR and Pyr in both summer and winter (Table 5). Five- and 6-ring PAHs require high-temperature combustion conditions, such as in gasoline and diesel engines, suggesting that PC1 was a traffic emission source (Harrison et al., 1996). Four-ring PAHs can be easily formed at relatively low combustion temperatures, such as that of coal and/or biomass combustion (Tang et al., 2005; Zhang et al., 2020c), suggesting that PC2 was coal burning. Consequently, the emission sources in Shanghai were mixed and were mainly affected by traffic sources, and some coal and/or biomass combustion occurred in summer and winter, consistent with the results of the diagnostic ratios.

Appendix A Table S4 summarizes the population, gross domestic product, motor vehicles, and energy consumption in Shanghai. The coal consumption supported the observed influence of coal combustion in Shanghai, as described above. Moreover, the consumption of energy (coal, gas and liquefied petroleum gas) decreased in recent years, which may be one of

Table 5 – Loading of nine individual PAHs in PM$_{\leq 2.1}$ by principal component analysis in summer and winter periods*.

	Summer		Winter	
	PC1	PC2	PC1	PC2
FR	0.37	**0.91**	0.34	**0.92**
Pyr	0.37	**0.89**	0.45	**0.86**
BaA	0.59	**0.71**	0.68	0.54
Chr	0.67	0.61	**0.80**	0.55
BbF	**0.74**	0.64	**0.87**	0.44
BkF	**0.84**	0.50	**0.91**	0.40
BaP	**0.92**	0.32	**0.88**	0.43
BgPe	**0.91**	0.39	**0.89**	0.37
IDP	**0.82**	0.48	**0.92**	0.34
Variance %	84.4%	7.67%	85.3%	7.75%

* High factor loadings (> 0.7) are marked in bold.

the most important reasons for the decreasing concentration of 4-ring PAHs in winter (Table 2), which mainly originate from incomplete coal burning (Harrison et al., 1996). Although the number of motor vehicles and the consumption of gasoline fuel and diesel oil have increased in recent years (**Appendix A Table S4**), the national standard for the emission limits for vehicles has become stricter. Specifically, the emission limit of PM was from 25 to 100 mg/km for different types of vehicles according to the national standard of the emission limits for light-duty vehicles issued in 2005 (GB18352.3–2005), while the emission limit was reduced to 4.5 mg/km for all types of vehicles in the new guideline issued in 2013 (GB18352.5–2013) and reduced to 3.0 mg/km in the newest guideline issued in 2016 (GB18352.6–2016). As shown in Table 2, the concentrations of 5- and 6-ring PAHs and 1-NP decreased in winter, indicating the positive effect of the new national standard because they easily originate from vehicle exhaust (Harrison et al., 1996; Tang et al., 2005). Comprehensively, in addition to the changes in energy consumption, such as reducing the use of fossil fuels, including coal, and increasing the use of clean energy, including natural gas, continually improving vehicle technology also controlled and reduced the emission of air pollutants, including PAHs and NPAHs in PM, from vehicle exhaust.

2.4. Backward trajectories

Backward trajectory analysis is used to determine the transport routes of the air mass (Tang et al., 2015; Yang et al., 2007, 2018; Zhang et al., 2020d). In this study, the results of the cluster analy-
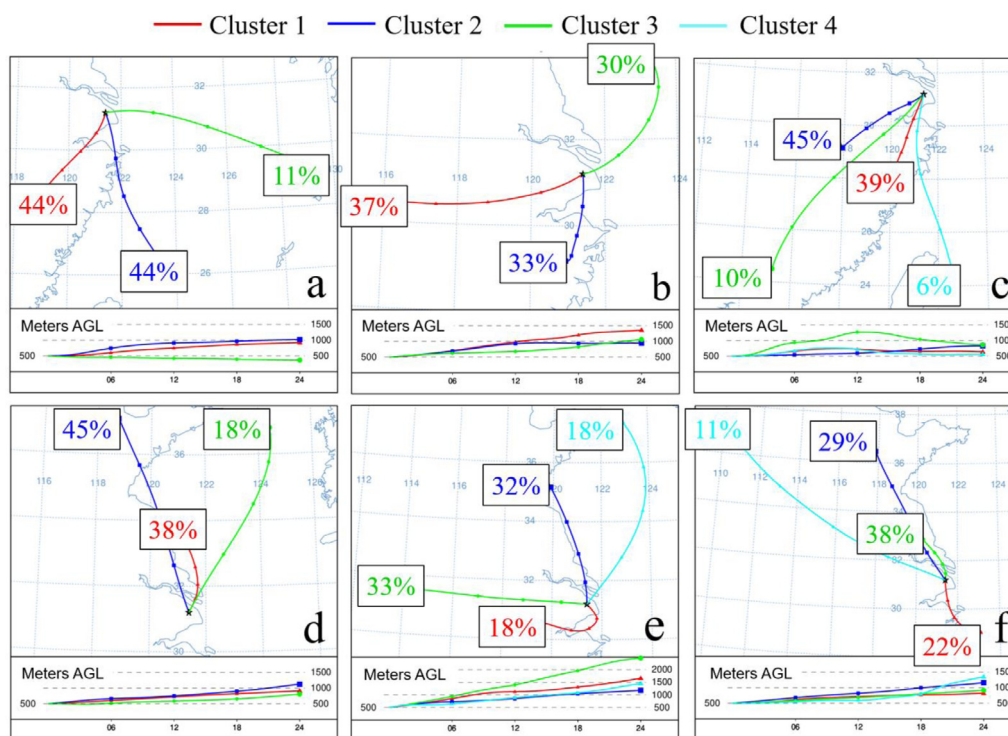
Fig. 2 – Cluster analysis of backward trajectories of air mass in summer (a: 2013; b: 2015; c: 2017) and winter (d: 2013; e: 2015; f: 2018).

sis of the backward trajectories in summer and winter are shown in Fig. 2. In summer (Fig. 2a-c), Shanghai is easily affected by air masses from the southern areas and the ocean, accounting for approximately 44% (cluster 1) and 55% (clusters 2 and 3) in 2013, 70% (clusters 1 and 2) and 30% (cluster 3) in 2015, and 94% (clusters 1, 2, and 3) and 6% (cluster 4) in 2017, respectively. In winter (Fig. 2d-f), most air masses come from the northern areas and surrounding areas, accounting for approximately 63% (clusters 2 and 3) and 38% (cluster 1) in 2013, 50% (clusters 2 and 4) and 18% (clusters 1 and 3) in 2015, and 40% (clusters 2 and 4) and 60% (clusters 1 and 3) in 2018, respectively. The air masses from the ocean can dilute some of the air pollutants in Shanghai (Liu et al., 2018; Wang et al., 2016b). Moreover, in addition to the influence of meteorological conditions described in Section 2.2, the residential heating systems in northern China released large amounts of PM from coal combustion (Ma et al., 2018), leading some PAHs and NPAHs in PM to be transported to Shanghai in winter. This was consistent with the previous study in which Liu et al. found that the relatively low concentration weighted trajectories towards Shanghai were in the southern areas and the ocean in summer and were in the central and northern areas in winter (Liu et al., 2018).

2.5. Health risks of PAHs and NPAHs

Table 6 summarizes the mean BaP_{eq} concentrations and the ILCR from 2010 to 2018. In this study, the mean BaP concentrations were all below the limit of the daily 24-hr standard (2.5 ng/m³) regulated by the national ambient air quality standard (GB3095–2012) (MEE, 2012). The BaP concentration in winter decreased gradually and remained 5.0 to 11.1 times higher than that in summer, indicating a relatively higher cancer risk in winter. The ΣBaP_{eq} concentrations also decreased in winter in recent years, similar to BaP. Table 6 indicates that BbF and IDP had the highest BaP_{eq} concentrations except for BaP, suggesting relatively higher health risks than the other PAHs. Moreover, although the con-

centrations of 1-NP and 2-NFR were much lower than those of PAHs (Table 2), Table 6 shows that the BaP_{eq} concentrations of 1-NP were comparable to those of FR and Pyr, and the BaP_{eq} concentrations of 2-NFR were comparable to Chr and BgPe due to the relatively higher TEF values of 1-NP and 2-NFR (Table 1).

As revealed in Table 6, the mean ILCR was the highest in 2010 (9.12×10^{-5}, which means that approximately 91 cancer cases can occur amongst one million people) and gradually decreased; the ILCR in 2017/2018 was the lowest (4.81×10^{-5}). Although the ILCR was one order of magnitude higher than the US EPA acceptable cancer risk level (10^{-6}), the ILCR in this study was over-amplified for ordinary people because the UR_{BaP} value used to calculate the ILCR was determined in an epidemiological study of coke-oven workers. Although the cancer risk in Shanghai still remains high, the decreasing trend in recent years suggests that the health risk of PAHs may foreseeably decrease in the future.

2.6. Research limitations

There were some limitations in the current research. Regarding sampling and source emission analysis, we did not collect gaseous samples, preventing the comparison of particle and gaseous phase PAHs and NPAHs. This also leads to some uncertainty in the diagnostic ratios and PCA results. Moreover, we did not analyse other US EPA priority PAHs, leading to some uncertainty in health risk assessment.

3. Conclusions

In this study, the regularly variations of the PM-bound PAHs and NPAHs in Shanghai over the past decade were first compared. The mean ΣPAHs and 1-NP concentrations in winter decreased by 39.7% and 79.0% from 2010 to 2018, respectively. BbF, BgPe, and 2-NFR were dominant compounds in all periods. The ambient

Table 6 – Mean BaP-equivalent concentrations (pg/m^3) and standard deviations of nine PAHs, 1-NP and 2-NFR in PM$_{\leq 2.1}$ and inhalation lifetime cancer risk (ILCR) from 2010 to 2018.

	2010[a]		2013		2015		2017/2018	
	Summer	Winter	Summer	Winter	Summer	Winter	Summer	Winter
FR	0.11 ± 0.05	1.17 ± 0.65	0.14 ± 0.05	2.06 ± 1.29	0.22 ± 0.11	1.57 ± 0.53	0.15 ± 0.04	1.39 ± 0.92
Pyr	0.12 ± 0.05	0.96 ± 0.46	0.13 ± 0.04	1.86 ± 1.06	0.22 ± 0.09	1.09 ± 0.32	0.11 ± 0.01	0.85 ± 0.58
BaA	5.48 ± 2.04	98.6 ± 44.5	5.77 ± 2.83	67.5 ± 45.8	7.33 ± 3.92	55.8 ± 25.5	6.44 ± 0.68	50.8 ± 29.0
Chr	1.05 ± 0.45	17.4 ± 7.64	1.16 ± 0.37	16.4 ± 10.2	1.11 ± 0.65	9.30 ± 4.36	0.87 ± 0.19	8.26 ± 3.95
BbF	29.3 ± 7.69	214 ± 84.4	21.2 ± 9.66	210 ± 123	34.5 ± 22.4	162 ± 80.0	26.9 ± 4.47	132 ± 43.0
BkF	11.1 ± 2.26	88.8 ± 30.5	7.19 ± 3.17	80.6 ± 47.2	10.6 ± 7.23	64.6 ± 31.9	6.63 ± 1.51	47.2 ± 16.0
BaP	151 ± 30.9	1270 ± 451	103 ± 45.1	1140 ± 734	122 ± 84.6	659 ± 361	115 ± 12.7	576 ± 248
BgPe	4.26 ± 1.28	21.9 ± 8.91	2.96 ± 1.38	25.3 ± 14.9	3.50 ± 2.48	13.9 ± 7.79	2.74 ± 0.48	9.78 ± 2.70
IDP	28.0 ± 9.04	145 ± 56.8	13.2 ± 6.15	136 ± 79.2	27.6 ± 19.0	105 ± 55.5	21.8 ± 4.74	79.6 ± 21.8
1-NP	0.63 ± 0.28	4.23 ± 1.61	0.35 ± 0.11	3.08 ± 1.54	0.19 ± 0.08	1.17 ± 0.64	0.43 ± 0.12	0.89 ± 0.21
2-NFR	-[b]	-[b]	-[b]	-[b]	4.65 ± 3.42	15.8 ± 10.6	8.68 ± 4.33	8.44 ± 3.51
ΣBaP$_{eq}$	231 ± 52.7	1860 ± 645	155 ± 67.6	1690 ± 1050	212 ± 142	1090 ± 567	190 ± 22.3	916 ± 363
ILCR	$(9.12 \pm 3.04) \times 10^{-5}$		$(8.00 \pm 4.88) \times 10^{-5}$		$(5.65 \pm 3.08) \times 10^{-5}$		$(4.81 \pm 1.67) \times 10^{-5}$	

[a] Concentration data from Tang et al., 2013.
[b] No concentration data.

temperature was found to affect PM-bound PAH and NPAH concentrations. The emission sources in Shanghai were mainly affected by traffic emissions with some coal and/or biomass combustion. The OH radical-initiated reaction was the main pathway for the secondary formation of 2-NP and 2-NFR. Moreover, the air mass routes were different in each period, and the effect of external sources from northern China was greater in winter. On the other hand, the mean ΣBaP$_{eq}$ concentrations and ILCR in winter both decreased in recent years.

A series of measures have been implemented to control air pollutant emissions from various sources in China in recent years. PAH and NPAH results in this study indicated the positive effects of various policies and regulations. However, the air pollution in winter is still severe. To further control and reduce air pollutant emissions, some measures should be strengthened. Examples include improving the combustion technology, such as increasing the combustion efficiency; popularizing the desulfurization and denitrification of fossil fuels; changing the energy structure, such as reducing the use of fossil fuels; popularizing clean and/or renewable energy; and using dust and smoke removal and condensation technologies to reduce some of the pollutants before entering the atmosphere. Moreover, the routes of exposure to PAHs and NPAHs include ingestion and dermal contact in addition to inhalation due to the characteristics of their generation and existence. Analysing simple and representative PAH and NPAH biomarkers can better evaluate the potential health risks of exposure to PAHs and NPAHs. However, the previous results of research on biomarkers, such as 1-hydroxypyrene in human urine (Chetiyanukornkul et al., 2006; Kim et al., 2013), still showed some shortcomings because absorption, metabolism, and excretion may differ amongst PAHs and NPAHs and vary significantly amongst humans. We hope that we can provide basic data for finding better PAH and NPAH biomarkers through the accumulation of our data from atmospheric observations.

Declaration of Competing Interest

The authors declare that they have no known competing financial interests or personal relationships that could have appeared to influence the work reported in this paper.

Acknowledgments

Appendix A. Supplementary data

Supplementary material associated with this article can be found, in the online version, at doi:10.1016/j.jes.2020.06.017.

REFERENCES

Albinet, A., Leoz-Garziandia, E., Budzinski, H., Villenave, E., Jaffrezo, J.-L., 2008. Nitrated and oxygenated derivatives of polycyclic aromatic hydrocarbons in the ambient air of two French alpine valleys: Part 1: Concentrations, sources and gas/particle partitioning. Atmos. Environ. 42, 43–54.

Amarillo, A.C., Carreras, H., 2016. Quantifying the influence of meteorological variables on particle-bound PAHs in urban environments. Atmos. Pollut. Res. 7, 597–602.

Arey, J., Zielinska, B., Atkinson, R., Winer, A.M., Ramdahl, T., Pitts, J.N., 1986. The formation of nitro-PAH from the gas-phase reactions of fluoranthene and pyrene with the OH radical in the presence of NOx. Atmos. Environ. 20, 2339–2345.

Baek, S., Field, R., Goldstone, M., Kirk, P., Lester, J., Perry, R., 1991. A review of atmospheric polycyclic aromatic hydrocarbons: sources, fate and behavior. Water Air Soil. Poll. 60, 279–300.

Bamford, H.A., Baker, J.E., 2003. Nitro-polycyclic aromatic hydrocarbon concentrations and sources in urban and suburban atmospheres of the Mid-Atlantic region. Atmos. Environ. 37, 2077–2091.

Byambaa, B., Yang, L., Matsuki, A., Nagato, E.G., Gankhuyag, K., Chuluunpurev, B., et al., 2019. Sources and characteristics of polycyclic aromatic hydrocarbons in ambient total suspended particles in Ulaanbaatar City, Mongolia. Int. J. Environ. Res. Public Health. 16, 442.

Chetiyanukornkul, T., Toriba, A., Kameda, T., Tang, N., Hayakawa, K., 2006. Simultaneous determination of urinary hydroxylated metabolites of naphthalene, fluorene, phenanthrene, fluoranthene and pyrene as multiple biomarkers of exposure to polycyclic aromatic hydrocarbons. Anal. Bioanal. Chem. 386 (3), 712–718.

Dunea, D., Iordache, S., Pohoata, A., 2016. Fine particulate matter in urban environments: a trigger of respiratory symptoms in sensitive children. Int. J. Environ. Res. Public Health. 13, 1246.

Durant, J.L., Busby Jr, W.F., Lafleur, A.L., Penman, B.W., Crespi, C.L., 1996. Human cell mutagenicity of oxygenated, nitrated and unsubstituted polycyclic aromatic hydrocarbons associated with urban aerosols. Mutat. Res. 371, 123–157.

Feng, B., Li, L., Xu, H., Wang, T., Wu, R., Chen, J., et al., 2019. PM$_{2.5}$-bound polycyclic aromatic hydrocarbons (PAHs) in Beijing: Seasonal variations, sources, and risk assessment. J. Environ. Sci. 77, 11–19.

Gu, Z., Feng, J., Han, W., Li, L., Wu, M., Fu, J., et al., 2010. Diurnal variations of polycyclic aromatic hydrocarbons associated with PM$_{2.5}$ in Shanghai, China. J. Environ. Sci. 22, 389–396.

Harrison, R.M., Smith, D., Luhana, L., 1996. Source apportionment of atmospheric polycyclic aromatic hydrocarbons collected from an urban location in Birmingham, UK. Environ. Sci. Technol. 30, 825–832.

Jiang, N., Li, Q., Su, F., Wang, Q., Yu, X., Kang, P., et al., 2018. Chemical characteristics and source apportionment of PM$_{2.5}$ between heavily polluted days and other days in Zhengzhou, China. J. Environ. Sci. 66, 188–198.

Kakimoto, H., Kitamura, M., Matsumoto, Y., Sakai, S., Kanoh, F., Murahashi, T., et al., 2000. Comparison of atmospheric polycyclic aromatic hydrocarbons and nitropolycyclic aromatic hydrocarbons in Kanazawa, Sapporo and Tokyo. J. Health Sci. 46, 5–15.

Kameda, T., Takenaka, N., Bandow, H., Inazu, K., Hisamatsu, Y., 2004. Determination of atmospheric nitro-polycyclic aromatic hydrocarbons and their precursors at a heavy traffic roadside and at a residential area in Osaka, Japan. Polycycl. Aromat. Comp. 24, 657–666.

Kim, K.-H., Jahan, S.A., Kabir, E., Brown, R.J., 2013. A review of airborne polycyclic aromatic hydrocarbons (PAHs) and their human health effects. Environ. Int. 60, 71–80.

Kong, S., Yan, Q., Zheng, H., Liu, H., Wang, W., Zheng, S., et al., 2018. Substantial reductions in ambient PAHs pollution and lives saved as a co-benefit of effective long-term PM$_{2.5}$ pollution controls. Environ. Int. 114, 266–279.

Liu, A., Qian, N., Yu, H., Chen, R., Kan, H., 2017. Estimation of disease burdens on preterm births and low birth weights attributable to maternal fine particulate matter exposure in Shanghai. China. Sci. Total Environ. 609, 815–821.

Liu, Y., Yu, Y., Liu, M., Lu, M., Ge, R., Li, S., et al., 2018. Characterization and source identification of PM$_{2.5}$-bound polycyclic aromatic hydrocarbons (PAHs) in different seasons from Shanghai, China. Sci. Total Environ. 644, 725–735.

Ma, W.-L., Liu, L.-Y., Jia, H.-L., Yang, M., Li, Y.-F., 2018. PAHs in Chinese atmosphere Part I: Concentration, source and temperature dependence. Atmos. Environ. 173, 330–337.

MEE (Ministry of Ecological Environment of the People's Republic of China), 2012. Ambient Air Quality Standard GB3095-2012. China Environmental Science Press, Beijing, China.

Nisbet, I.C., Lagoy, P.K., 1992. Toxic equivalency factors (TEFs) for polycyclic aromatic hydrocarbons (PAHs). Regul. Toxicol. Pharm. 16, 290–300.

OEHHA (Office of Environmental Health Hazard Assessment), 2005. Air Toxics Hot Spots Program Risk Assessment Guidelines. Part II Technical Support Document for Describing Available Cancer Potency Factors. California Environmental Protection Agency, Office of Environmental Health Hazard Assessment, Air Toxicology and Epidemiology Section.

Polachova, A., Gramblicka, T., Parizek, O., Sram, R.J., Stupak, M., Hajslova, J., et al., 2020. Estimation of human exposure to polycyclic aromatic hydrocarbons (PAHs) based on the dietary and outdoor atmospheric monitoring in the Czech Republic. Environ. Res. 182, 108977.

Ravindra, K., Sokhi, R., Van Grieken, R., 2008. Atmospheric polycyclic aromatic hydrocarbons: source attribution, emission factors and regulation. Atmos. Environ. 42, 2895–2921.

Rogge, W.F., Hildemann, L.M., Mazurek, M.A., Cass, G.R., Simoneit, B.R., 1993. Sources of fine organic aerosol. 2. Noncatalyst and catalyst-equipped automobiles and heavy-duty diesel trucks. Environ. Sci. Technol. 27, 636–651.

Simcik, M.F., Eisenreich, S.J., Lioy, P.J., 1999. Source apportionment and source/sink relationships of PAHs in the coastal atmosphere of Chicago and Lake Michigan. Atmos. Environ. 33, 5071–5079.

Taga, R., Tang, N., Hattori, T., Tamura, K., Sakai, S., Toriba, A., et al., 2005. Direct-acting mutagenicity of extracts of coal burning-derived particulates and contribution of nitropolycyclic aromatic hydrocarbons. Mutat. Res. 581, 91–95.

Tang, N., Hattori, T., Taga, R., Igarashi, K., Yang, X.Y., Tamura, K., et al., 2005. Polycyclic aromatic hydrocarbons and nitropolycyclic aromatic hydrocarbons in urban air particulates and their relationship to emission sources in the Pan–Japan Sea countries. Atmos. Environ. 39, 5817–5826.

Tang, N., Tokuda, T., Izzaki, A., Tamura, K., Ji, R., Zhang, X., et al., 2011. Recent changes in atmospheric polycyclic aromatic hydrocarbons (PAHs) and nitropolycyclic aromatic hydrocarbons (NPAHs) in Shenyang, China. Environ. Forensics 12, 342–348.

Tang, N., Izzaki, A., Tokuda, T., Ji, R., Dong, L., Wu, Q., et al., 2013. Characteristics of atmospheric polycyclic aromatic hydrocarbons in Shenyang, Shanghai and Fuzhou, China. Bunseki Kagaku 62, 267–273.

Tang, N., Sato, K., Tokuda, T., Tatematsu, M., Hama, H., Suematsu, C., et al., 2014. Factors affecting atmospheric 1- 2-nitropyrenes and 2-nitrofluoranthene in winter at Noto peninsula, a remote background site, Japan. Chemosphere 107, 324–330.

Tang, N., Hakamata, M., Sato, K., Okada, Y., Yang, X.Y., Tatematsu, M., et al., 2015. Atmospheric behaviors of polycyclic aromatic hydrocarbons at a Japanese remote background site, Noto peninsula, from 2004 to 2014. Atmos. Environ. 120, 144–151.

Tang, N., Suzuki, G., Morisaki, H., Tokuda, T., Yang, X.Y., Zhao, L.X., et al., 2017. Atmospheric behaviors of particulate-bound polycyclic aromatic hydrocarbons and nitropolycyclic aromatic hydrocarbons in Beijing, China from 2004–2010. Atmos. Environ. 152, 354–361.

Wang, W., Jing, L., Zhan, J., Wang, B., Zhang, D., Zhang, H., et al., 2014. Nitrated polycyclic aromatic hydrocarbon pollution during the Shanghai World Expo 2010. Atmos. Environ. 89, 242–248.

Wang, J., Li, X., Jiang, N., Zhang, W., Zhang, R., Tang, X., 2015. Long term observations of PM$_{2.5}$-associated PAHs: comparisons between normal and episode days. Atmos. Environ. 104, 228–236.

Wang, Q., Liu, M., Yu, Y., Li, Y., 2016a. Characterization and source apportionment of PM$_{2.5}$-bound polycyclic aromatic hydrocarbons from Shanghai city, China. Environ. Pollut. 218, 118–128.

Wang, H., Qiao, L., Lou, S., Zhou, M., Ding, A., Huang, H., et al., 2016b. Chemical composition of PM$_{2.5}$ and meteorological impact among three years in urban Shanghai, China. J. Clean. Prod. 112, 1302–1311.

Wang, T., Xia, Z., Wu, M., Zhang, Q., Sun, S., Yin, J., et al., 2017. Pollution characteristics, sources and lung cancer risk of atmospheric polycyclic aromatic hydrocarbons in a new urban district of Nanjing, China. J. Environ. Sci. 55, 118–128.

Wang, W., Liu, C., Ying, Z., Lei, X., Wang, C., Huo, J., et al., 2019. Particulate air pollution and ischemic stroke hospitalization: How the associations vary by constituents in Shanghai, China. Sci. Total Environ. 695, 133780.

WHO (World Health Organization), 2000. Air Quality Guidelines for Europe, Part II Evaluation of Risks to Human Health, Chapter 5 Organic Pollutants European Series No. 91.

Xing, W.L., Zhang, L.L., Yang, L., Zhou, Q.Y., Zhang, X., Toriba, A., et al., 2020. Characteristics of PM$_{2.5}$-bound polycyclic aromatic hydrocarbons and nitro-polycyclic aromatic hydrocarbons at a roadside air pollution monitoring station in Kanazawa, Japan. Int. J. Environ. Res. Public Health. 17, 805.

Yamasaki, H., Kuwata, K., Miyamoto, H., 1982. Effects of ambient temperature on aspects of airborne polycyclic aromatic hydrocarbons. Environ. Sci. Technol. 16, 189–194.

Yan, L., Li, X., Chen, J., Wang, X., Du, J., Ma, L., 2012. Source and deposition of polycyclic aromatic hydrocarbons to Shanghai. China. J. Environ. Sci. 24, 116–123.

Yang, X.Y., Okada, Y., Tang, N., Matsunaga, S., Tamura, K., Lin, J.M., et al., 2007. Long-range transport of polycyclic aromatic hydrocarbons from China to Japan. Atmos. Environ. 41, 2710–2718.

Yang, L., Tang, N., Matsuki, A., Takami, A., Hatakeyama, S., Kaneyasu, N., et al., 2018. A Comparison of particulate-bound polycyclic aromatic hydrocarbons long-range transported from the Asian continent to the Noto Peninsula and Fukue Island, Japan. Asian J. Atmos. Environ. 12, 369–376.

Yang, L., Suzuki, G., Zhang, L.L., Zhou, Q.Y., Zhang, X., Xing, W.L., et al., 2019. The characteristics of polycyclic aromatic hydrocarbons in different emission source areas in Shenyang, China. Int. J. Environ. Res. Public Health. 16, 2817.

Yunker, M.B., Macdonald, R.W., Vingarzan, R., Mitchell, R.H., Goyette, D., Sylvestre, S., 2002. PAHs in the Fraser River basin: a critical appraisal of PAH ratios as indicators of PAH source and composition. Org. Geochem. 33, 489–515.

Zhang, L.L., Morisaki, H., Wei, Y.J., Li, Z.G., Yang, L., Zhou, Q.Y., et al., 2020b. PM$_{2.5}$-bound polycyclic aromatic hydrocarbons and nitro-polycyclic aromatic hydrocarbons inside and outside a primary school classroom in Beijing: Concentration, composition, and inhalation cancer risk. Sci. Total Environ. 705, 135840.

Zhang, L.L., Tokuda, T., Yang, L., Zhou, Q.Y., Zhang, X., Xing, W.L., et al., 2019b. Characteristics and health risks of particulate polycyclic aromatic hydrocarbons and nitro-polycyclic aromatic hydrocarbons at urban and suburban elementary schools in Shanghai, China. Asian J. Atmos. Environ. 13, 266–275.

Zhang, L.L., Morisaki, H., Wei, Y.J., Li, Z.G., Yang, L., Zhou, Q.Y., et al., 2019a. Characteristics of air pollutants inside and outside a primary school classroom in Beijing and respiratory health impact on children. Environ. Pollut. 255, 113147.

Zhang, Y., Yang, L., Zhang, X., Li, J., Zhao, T., Gao, Y., et al., 2019d. Characteristics of PM$_{2.5}$-bound PAHs at an urban site and a suburban site in Jinan in North China Plain. Aerosol Air Qual. Res. 19, 871–884.

Zhang, L.L., Yang, L., Zhou, Q.Y., Zhang, X., Xing, W.L., Wei, Y.J., et al., 2020c. Size distribution of particulate polycyclic aromatic hydrocarbons in fresh combustion smoke and ambient air: A review. J. Environ. Sci. 88, 370–384.

Zhang, L.L., Zhang, X., Xing, W.L., Zhou, Q.Y., Yang, L., Nakatsubo, R., et al., 2020a. Natural aeolian dust particles have no substantial effect on atmospheric polycyclic aromatic hydrocarbons (PAHs): A laboratory study based on naphthalene. Environ. Pollut. 263, 114454.

Zhang, X., Zhang, L.L., Yang, L., Zhou, Q.Y., Xing, W.L., Toriba, A., et al., 2020d. Characteristics of Polycyclic Aromatic Hydrocarbons (PAHs) and Common Air Pollutants at Wajima, a Remote Background Site in Japan. Int. J. Environ. Res. Public Health. 17, 957.

Zhang, Y., Zheng, H., Zhang, L., Zhang, Z., Xing, X., Qi, S., 2019c. Fine particle-bound polycyclic aromatic hydrocarbons (PAHs) at an urban site of Wuhan, central China: characteristics, potential sources and cancer risks apportionment. Environ. Pollut. 246, 319–327.

Zielinska, B., Arey, J., Atkinson, R., Winer, A.M., 1989. The nitroarenes of molecular weight 247 in ambient particulate samples collected in southern California. Atmos. Environ. 23, 223–229.